

# Bowl vs Saddle Conformations in Cyclononatriene-Based Anion Binding Hosts

Mara Staffilani, Giuliana Bonvicini, and Jonathan W. Steed\*

Department of Chemistry, King's College London, Strand, London WC2R 2LS, U.K.

K. Travis Holman and Jerry L. Atwood

Department of Chemistry, University of Missouri–Columbia, Columbia, Missouri 65211

Mark R. J. Elsegood

Department of Chemistry, Bedson Building, University of Newcastle upon Tyne, Newcastle upon Tyne NE1 7RU, U.K.

Received August 19, 1997

The synthesis of organometallic complexes  $[\{\text{Ru}(p\text{-MeC}_6\text{H}_4\text{CHMe}_2)\}_n(\text{C}_{21}\text{H}_{24}\text{S}_3)][\text{CF}_3\text{SO}_3]_{2n}$  ( $n = 1$ , **6**;  $n = 2$ , **7**) and  $[\{\text{Ir}(\text{C}_5\text{Me}_5)\}_2(\text{C}_{21}\text{H}_{24}\text{S}_3)][\text{CF}_3\text{SO}_3]_4$  (**9**) based upon the trimeric macrocycle cyclotris(dimethylthiophenylene) (**4**) is reported. A saddle conformation is identified for the free ligand **4** and complexes **6** and **9** by X-ray crystallography. The anion complexation behavior of complex **9** is compared with the related cyclotrimeratrylene complex  $[\{\text{Ru}(p\text{-MeC}_6\text{H}_4\text{CHMe}_2)\}_2(\text{C}_{27}\text{H}_{30}\text{O}_6)][\text{CF}_3\text{SO}_3]_4$  (**2**), which possesses a bowl-shaped conformation, by  $^1\text{H}$  NMR titration studies in a variety of solvents. While host **2** displays a significant affinity for halides with binding constants of up to  $1.25(7) \times 10^3 \text{ M}^{-1}$  in nitromethane solution, the absence of a molecular cavity in **9** results in very little specific anion affinity. The 1,3-alternate calix[4]arene complex  $[\{\text{Ru}(\eta^6\text{-}p\text{-MeC}_6\text{H}_4\text{CHMe}_2)\}_2(\eta^6\text{:}\eta^6\text{-C}_{40}\text{H}_{48})][\text{BF}_4]_4$  (**11**) is also reported and shown to bind anions in an unusual C–H $\cdots$ anion hydrogen-bonding fashion by X-ray crystallography and  $^1\text{H}$  NMR.

## Introduction

The design of new host materials for anionic guests is of growing importance despite the difficulties associated with their design and has been the subject of several recent reviews.<sup>1–7</sup> In particular, anion-selective hosts show a great deal of promise in the development of novel sensor devices for environmentally important anions such as nitrate and phosphate or as anion sensors in biological systems.<sup>2,4,8–10</sup> Host molecules which display even partial anion selectivity may be incorporated into an electrode polymer membrane or directly attached to an electrode surface to give a selective anion response. Microsensor arrays of such devices of differing selectivities would give a characteristic signature for anionic species of interest.

We have previously reported a range of anion-binding hosts based upon transition-metal complexes of cyclotrimeratrylene (CTV, **1**)<sup>11</sup> in which anionic guests are included within the host<sup>12</sup> as a result of electrostatic attraction to the partially positively charged aromatic rings,<sup>13</sup> e.g.,  $[\{\text{Ru}(\eta^6\text{-}p\text{-MeC}_6\text{H}_4\text{CHMe}_2)\}_2(\eta^6\text{:}\eta^6\text{-CTV})][\text{CF}_3\text{SO}_3]_4$  (**2**) and  $[\{\text{Ru}(\eta^6\text{-}p\text{-MeC}_6\text{H}_4\text{CHMe}_2)\}_3(\eta^6\text{:}\eta^6\text{:}\eta^6\text{-CTV})][\text{BF}_4]_6$  (**3**), both of which have been shown by X-ray crystallography to include anionic guests within the host molecular cavity.<sup>14–17</sup> It has been suggested that the degree of discrimination between anions by the host cation may result from size match considerations between the dimensions of the host cavity and those of the anion (although, clearly, factors such as solvation energy and binding to anions outside of the cavity are also highly important<sup>15,16</sup>). Thus, the anions which best fit the cavity will be able to sit closest to the cationic

\* Author to whom correspondence should be addressed. E-mail: jon.steed@kcl.ac.uk.

(1) Gale, P. A.; Sessler, J. L.; Kral, V. *Chem. Commun.* **1998**, 1–8.

(2) Beer, P. D. *J. Chem. Soc., Chem. Commun.* **1996**, 689–696.

(3) Lehn, J.-M. *Supramolecular Chemistry*, 1st ed.; VCH: Weinheim, Germany, 1995.

(4) Czarnik, A. W. *Acc. Chem. Res.* **1994**, *27*, 302–308.

(5) Dietrich, B. *Pure Appl. Chem.* **1993**, *65*, 1457–1464.

(6) *Supramolecular Chemistry of Anions*; Bowman-James, K., Bianchi, A., Garcia-Espana, E., Eds.; Wiley-VCH: Weinheim, Germany, 1997.

(7) Holman, K. T.; Atwood, J. L.; Steed, J. W. *Supramolecular Anion Receptors*. In *Advances in Supramolecular Chemistry*; Gokel, G., Ed.; JAI Press: London, 1997; Vol. 4, pp 287–331.

(8) Fabbrizzi, L.; Poggi, A. *Chem. Soc. Rev.* **1995**, 197–202.

(9) Mason, C. F. *Biology of Freshwater Pollution*, 2nd ed.; Longman: Harlow, U.K., 1991.

(10) Freiser, H. *Ion Selective Electrodes in Analytical Chemistry*; Freiser, H., Ed.; Plenum Press: New York, 1978; Vol. 1.

(11) Collet, A. *Tetrahedron* **1987**, *43*, 5725.

(12) Staffilani, M.; Hancock, K. S. B.; Steed, J. W.; Holman, K. T.; Atwood, J. L.; Juneja, R. K.; Burkhalter, R. S. *J. Am. Chem. Soc.* **1997**, *119*, 6324–6335.

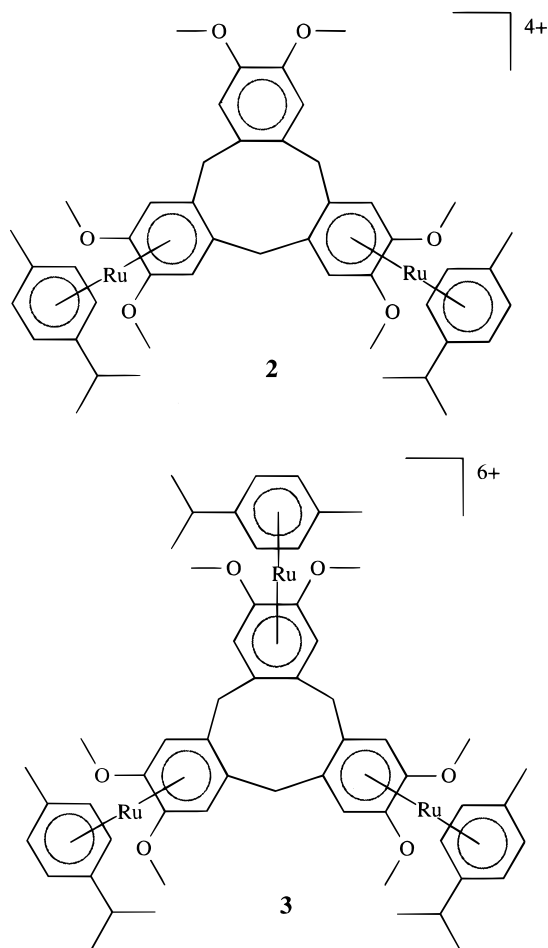
(13) Davies, S. G.; Green, M. L. H.; Mingos, D. M. P. *Tetrahedron* **1978**, *34*, 3047–3077.

(14) Steed, J. W.; Junk, P. C.; Atwood, J. L.; Barnes, M. J.; Raston, C. L.; Burkhalter, R. L. *J. Am. Chem. Soc.* **1994**, *116*, 10346–10347.

(15) Mitchell, A. B.; Steed, J. W.; Holman, K. T.; Halihan, M. M.; Montgomery, J.; Jurisson, S. S.; Atwood, J. L.; Burkhalter, R. S. *J. Am. Chem. Soc.* **1996**, *118*, 9567–9576.

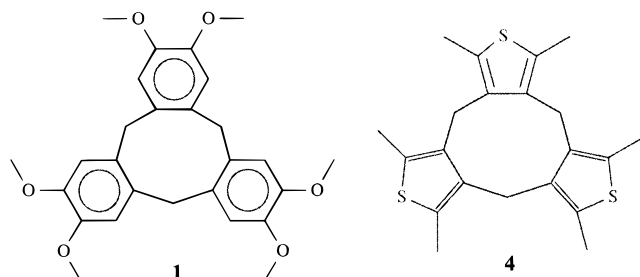
(16) Holman, K. T.; Halihan, M. M.; Steed, J. W.; Jurisson, S. S.; Atwood, J. L. *J. Am. Chem. Soc.* **1995**, *117*, 7848–7849.

(17) Atwood, J. L.; Holman, K. T.; Steed, J. W. *J. Chem. Soc., Chem. Commun.* **1996**, 1401–1407.



metal centers, maximizing anion–host electrostatic interactions.

To assess the importance of the cavity in hosts such as **2** and **3**, we now report the synthesis and anion complexation behavior of organometallic derivatives of the thiophene-based macrocycle hexamethylcyclotriphenylene **4**,<sup>18</sup> which, while it has the same core nine-membered ring structure as CTV, adopts a flexible saddle-shaped conformation in solution as a consequence of unfavorable steric interactions between the methyl substituents, Figure 1.



## Results and Discussion

**Synthesis and Structure.** Treatment of  $[\{\text{Ru}(\eta^6\text{-}p\text{-MeC}_6\text{H}_4\text{CHMe}_2)\text{Cl}(\mu\text{-Cl})\}_2]$  (**5**) with  $\text{AgCF}_3\text{SO}_3$  followed by reaction with 2 equiv of compound **4** gave the monometallic complex  $[\text{Ru}(\eta^6\text{-}p\text{-MeC}_6\text{H}_4\text{CHMe}_2)(\eta^5\text{-C}_{21}\text{H}_{24}\text{S}_3)]\text{[CF}_3\text{SO}_3\text{]}_2$  (**6**) in 82% yield. The complex was characterized on the basis of elemental analysis, FAB

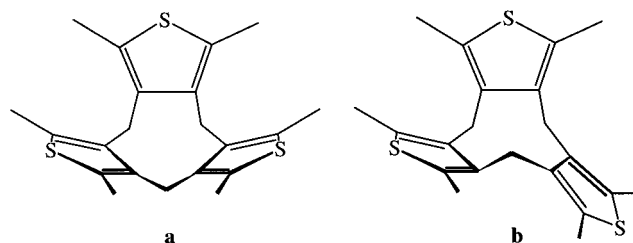


**Figure 1.** Bowl (a) and saddle (b) conformations of ligand **4** and its derivatives.

mass spectrometry (observed  $m/z = 757 \text{ M}^+ + \text{CF}_3\text{SO}_3$ ,  $608 \text{ M}^+$ ), and  $^1\text{H}$  NMR spectroscopy. Similarly, reaction of a 1:1 mole ratio of **5** and **4** resulted in the formation of the bimetallic compound  $[\{\text{Ru}(\eta^6\text{-}p\text{-MeC}_6\text{H}_4\text{CHMe}_2)\}_2(\eta^5\text{-}\eta^5\text{-C}_{21}\text{H}_{24}\text{S}_3)]\text{[CF}_3\text{SO}_3\text{]}_4$  (**7**) (FAB-MS  $m/z = 1292 \text{ M}^+ + 3\text{CF}_3\text{SO}_3$ ,  $1143 \text{ M}^+ + 2\text{CF}_3\text{SO}_3$ ,  $994 \text{ M}^+ + \text{CF}_3\text{SO}_3$ ). Related complexes of 2,5-dimethylthiophene have been prepared previously.<sup>19</sup> The  $^1\text{H}$  NMR data of complexes **6** and **7** are given in Table 1. In both cases, some or all of the resonances due to the methylene bridges of the central nine-membered ring occur as AB quartets with geminal coupling constants of ca. 16 Hz. This is consistent with the results observed for **1**, **2**, and **3**, which have a stable bowl conformation, but is in contrast with the  $^1\text{H}$  NMR spectrum of free **4** where a singlet signal is observed, indicating rapid interconversion between bowl and saddle conformations, Figure 1.<sup>18</sup> Clearly, addition of the bulky (arene) $\text{Ru}^{2+}$  fragments to the macrocycle has the effect of freezing out the conformational equilibrium. This was confirmed by examination of the  $^1\text{H}$  NMR spectrum at various temperatures. No change was observed down to 193 K in acetone- $d_6$ . A similar effect has been noted by us for related complexes of cyclotetraveratrylene (CTTV).<sup>15</sup> In the case of CTV derivatives such as **2** and **3**, the bowl conformation (similar to Figure 1a) is the only one observed both crystallographically and in solution.<sup>14–17</sup> For **6**, the present  $^1\text{H}$  NMR data does not distinguish between a bowl and saddle conformation. For the bimetallic complex **7**, however, the only way in which a singlet signal can be observed for the methylene protons  $\text{H}_b$ , Figure 2, is for the two metal centers to be situated upon the opposite faces of the macrocycle to give an approximate 2-fold rotation axis passing through the methylene carbon atom  $\text{C}_b$  and the sulfur of the uncomplexed thiophene ring, implying a saddle conformation. Surprisingly, however, two sets of signals for the *p*-cymene spectator ligands are observed, suggesting a slight inequivalence of the two rings, possibly arising from the conformation of the macrocycle or unsymmetrical anion–host interactions.

Attempts to prepare pure samples of complex **7** were frustrated by the compound's tendency to retain solvent (particularly  $\text{CF}_3\text{CO}_2\text{H}$  and adventitious water). Attempts to dry the solid complex even at temperatures as low as 60 °C resulted in partial decomposition to another species having *p*-cymene resonances at ca. 5.9–6.1 ppm. These signals also appeared upon warming the sample to 50 °C in nitromethane in an NMR tube. Refluxing the sample overnight in acetone did not result in any decomposition, however, similar overnight reflux

(18) Meth-Cohn, O. *Tetrahedron Lett.* **1973**, 91–94.

(19) Russell, M. J. H.; White, C. A. Y.; Maitlis, P. M. *J. Chem. Soc., Dalton Trans.* **1978**, 857–861.

**Table 1.**  $^1\text{H}$  NMR Data for the New Complexes<sup>a</sup>

compound	H <sub>a</sub>	H <sub>b</sub>	H <sub>c</sub> –H <sub>e</sub>	<i>p</i> -cymene or C <sub>5</sub> Me <sub>5</sub>
[Ru(MeC <sub>6</sub> H <sub>4</sub> CHMe <sub>2</sub> )(C <sub>21</sub> H <sub>24</sub> S <sub>3</sub> )](CF <sub>3</sub> SO <sub>3</sub> ) <sub>2</sub> ( <b>6</b> )	3.99, 3.93 (AB, 2H, <sup>2</sup> J 16.0)	3.80, 3.15 (AB, 2H, <sup>2</sup> J 16.5)	2.53 (s, 6H), 2.48 (s, 6H), 2.23 (s, 6H)	6.93, 6.81 (AB, 4H, <sup>3</sup> J 6.7), 3.12 (sp, 1H, <sup>3</sup> J 6.9), 2.53 (s, 3H), 1.46 (d, 6H, <sup>3</sup> J 6.9)
[{Ru(MeC <sub>6</sub> H <sub>4</sub> CHMe <sub>2</sub> ) <sub>2</sub> (C <sub>21</sub> H <sub>24</sub> S <sub>3</sub> )](CF <sub>3</sub> SO <sub>3</sub> ) <sub>4</sub> ( <b>7</b> )	3.86, 3.78 (AB, 4H, <sup>2</sup> J 16.8)	4.78 (s, 2H)	2.87 (s, 6H), 2.45 (s, 6H), 2.29 (s, 6H)	7.05, 6.95 (AB, 4H, <sup>3</sup> J 5.9), 7.03, 6.91 (AB, 4H, <sup>3</sup> J 6.7), 3.20 (sp, 1H, <sup>3</sup> J 6.9), 2.60 (s, 6H), 1.46 (d, 6H, <sup>3</sup> J 6.9), 1.45 (d, 6H, <sup>3</sup> J 6.9)
[{Ir(C <sub>5</sub> Me <sub>5</sub> ) <sub>2</sub> (C <sub>21</sub> H <sub>24</sub> S <sub>3</sub> )](CF <sub>3</sub> SO <sub>3</sub> ) <sub>4</sub> ( <b>9</b> )	3.93, 3.58 (AB, 4H, <sup>2</sup> J 17.1)	4.39 (s, 2H)	2.92 (s, 6H), 2.45 (s, 6H), 2.33 (s, 6H)	2.40 (s, 30H)
[{Ru(MeC <sub>6</sub> H <sub>4</sub> CHMe <sub>2</sub> ) <sub>2</sub> (C <sub>40</sub> H <sub>48</sub> )](BF <sub>4</sub> ) <sub>4</sub> ( <b>11</b> )	7.08 (s, 2H), 6.99 (s, 2H), 4.29, 4.13 (AB, 8H, <sup>2</sup> J 17.5), 2.73 (s, 12H), 2.44 (s, 12H), 1.55 (s, 6H), 1.25 (s, 6H)			6.85, 6.76 (AB, 8H, <sup>3</sup> J 6.6), 3.08 (sp, 2H, <sup>3</sup> J 6.9), 2.57 (s, 6H), 1.45 (d, 12H, <sup>3</sup> J 6.9)

<sup>a</sup> At 350 MHz,  $\delta$  in ppm, *J* in hertz, solvent CD<sub>3</sub>NO<sub>2</sub>, and at 20 °C.

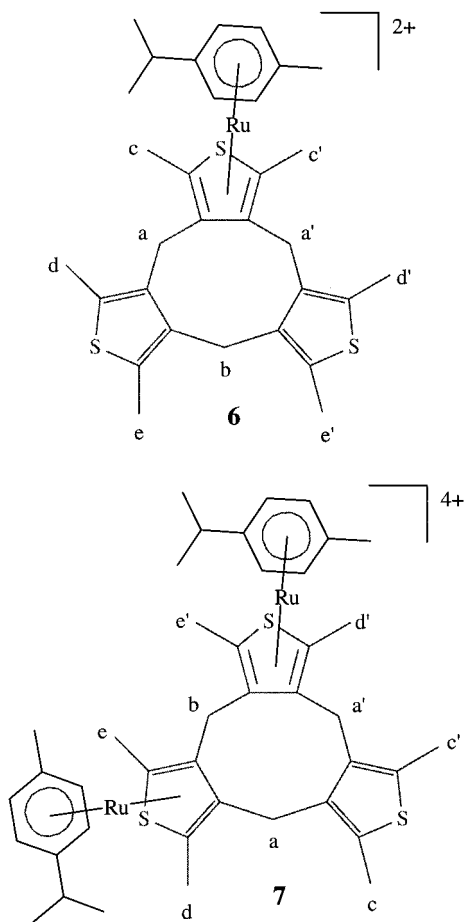


**Figure 2.**  $^1\text{H}$  NMR assignment scheme for complexes **6** and **7**. A similar scheme to that adopted for **7** is used for **9**.

of **7** in nitromethane solution resulted in its complete conversion into **6**. We surmise that the sterically crowded nature of a bimetallic species such as **7** makes it particularly susceptible to decomplexation of one of the organometallic fragments in the presence of a strongly coordinating solvent, possibly via an  $\eta^4$ -intermediate.<sup>19</sup>

Following an analogous procedure to that adopted for the synthesis of **7**, starting from [ $\{\text{Ir}(\eta^5\text{-C}_5\text{Me}_5)\text{Cl}(\mu\text{-Cl})\}_2$ ] (**8**),<sup>20</sup> the bimetallic iridium complex [ $\{\text{Ir}(\eta^5\text{-C}_5\text{Me}_5)_2(\eta^5\text{-}\eta^5\text{-C}_{21}\text{H}_{24}\text{S}_3)\}(\text{CF}_3\text{SO}_3)_4$ ] (**9**) (FAB-MS *m/z* = 1028  $\text{M}^+$ ) was also prepared. The  $^1\text{H}$  NMR spectrum of **9** (Table 1) also displayed a singlet for methylene protons H<sub>b</sub>, indicating a saddle conformation. In

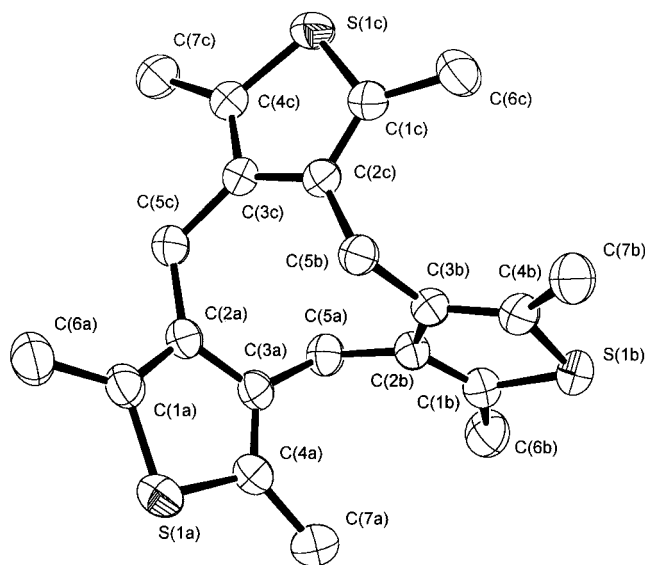


**Figure 3.** X-ray crystal structure of the ligand **4**.

this case, only one signal was observed for the C<sub>5</sub>Me<sub>5</sub> spectator ligands.

Attempts were also made to prepare trimetallic derivatives analogous to compound **3**, however, only bimetallic species were isolated even after prolonged reflux with large excesses of **5** and **8**. From examination of molecular models, it seems likely that a trimetallic complex would be extremely sterically hindered.

Given the interesting conformational properties of **4** and complexes **6**, **7**, and **9** as well as the potential of **7** and **9**, especially, to act as anion-binding hosts, we decided to carry out a series of X-ray crystal structure investigations. Crystals of the free ligand **4** were prepared by vacuum sublimation of the compound, and the X-ray structure is shown in Figure 3. In fact, the molecule possesses a noncrystallographic 2-fold rotation axis passing through S(1B) and C(5C) which relates ring A (defined as the pentagon containing S(1A) and C(1A)–C(4A)) to ring C. This results in a relatively rigid, symmetrical structure in which unfavorable steric interactions between the methyl substituents are minimized. There is, however, still a significant amount of strain in the central nine-membered ring, with angles subtended at the methylene bridges C(5A) and C(5B)

(20) Kang, J. W.; Moseley, K.; Maitlis, P. M. *J. Am. Chem. Soc.* **1969**, *91*, 5970.

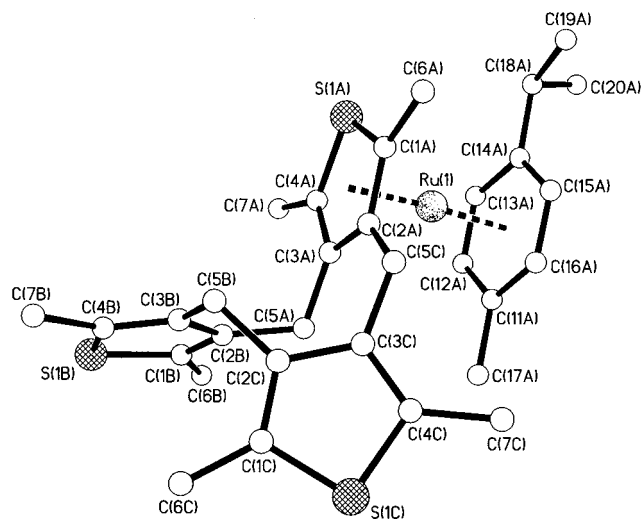


**Figure 4.** X-ray crystal structure of the monometallic cation in **6** showing the saddle conformation for the ligand **4**.

of  $112.3(2)^\circ$  and  $113.2(2)^\circ$  while that at C(5C) is remarkable at  $121.2(2)^\circ$ . This represents significantly more ring strain than observed for CTV itself, which exhibits angles at the methylenic bridges of between  $108.5(4)^\circ$  and  $116.4(5)^\circ$ .<sup>21</sup> The remaining bond lengths and angles are unremarkable. In the solid state, the molecules pack one above the other in the crystallographic *b* direction in a fashion reminiscent of CTV.<sup>21</sup>

In general, the bimetallic complexes **7** and **9** proved to be poorly crystalline as a consequence of their tendency to retain solvent molecules (especially  $\text{CF}_3\text{-CO}_2\text{H}$  and adventitious water, as evidenced by their  $^1\text{H}$  NMR spectra). The first crystals isolated proved to consist of the sulfido-bridged trimetallic species  $[\{\text{Ir}(\eta^5\text{-C}_5\text{Me}_5)\}_3(\mu_3\text{-S})][\text{BF}_4]_2$  previously reported by Niskioka and Isobe,<sup>22</sup> apparently arising from decomposition of the tetrafluoroborate salt of **9**, possibly *via* a hydrodesulfurization mechanism,<sup>23</sup> while being recrystallized over a period of weeks from dimethylformamide (dmf). Eventually, however, crystals of both **6** and **9** were prepared by slow cooling of the reaction mixture (**6**) or slow diffusion of diethyl ether vapor into a dmf solution of **9** and were analyzed by X-ray crystallography at  $-113^\circ\text{C}$ .

The crystal structure of **6**, Figure 4, shows a saddle conformation for the macrocyclic ligand very similar to that of **4** with intercentroid contacts A–B 4.51 Å, A–C 4.78 Å, B–C 4.43 Å, and hence, there is no molecular cavity available for anion binding. Ru–C<sub>cymene</sub> distances fall into the range 2.203(2)–2.257(2) Å and are unremarkable.<sup>24</sup> Ru–C<sub>thiophene</sub> distances fall into the range 2.184(2)–2.251(2) Å with slightly shorter bonds to the carbon atoms attached to sulfur, C(1A) and C(4A). The Ru–S bond length of 2.3432(6) Å is fully consistent with an  $\eta^5$ -description of the bonding, cf. 2.97 Å for the  $\eta^4$ -complex  $[\text{Ir}(\eta^5\text{-C}_5\text{Me}_5)(\eta^4\text{-SC}_4\text{H}_2\text{Me}_2)]^+$ .<sup>25</sup> Within the thiophene ligand, longer S–C bonds (1.745(2) Å (aver-

age) are observed for the coordinated ring, A [S(1A)–C(4A)], than the remaining rings, B [S(1B)–C(4B)] and C [S(1C)–C(4C)], 1.726(3) Å (average), consistent with a weakening of the S–C bonds as a consequence of  $d\text{-}\pi^*$  back-donation (cf. **4** 1.718(3) Å (average)). As for **4**, bond angles at the methylene bridging carbon atoms are somewhat larger than the ideal  $109.5^\circ$ , suggesting strain in the central nine-membered ring. The angle at C(5C) of  $118.3(2)^\circ$  is particularly large, again reflecting the conflict in attempting to relieve ring strain and simultaneously minimize unfavorable  $\text{CH}_3\text{-CH}_3$  interactions. For comparison, the analogous angles in  $[\text{Ru}(p\text{-cymene})\text{-}(\text{CTV})][\text{BF}_4]_2$  fall in the range  $109.9\text{--}112.6^\circ$ .<sup>15</sup> The ligand conformation is closely related to that of **4** despite the presence of the bulky metal center on one side of the ligand pseudo-2-fold axis. The metal center does, however, cause a marked deviation from the more symmetrical ligand **4** in respect to the torsion angles across the methylene bridge C(5C). In particular, the C(2C)–C(3C) and C(5C)–C(2A) bonds are almost eclipsed in **4** whereas they exhibit a torsion angle of  $-59.2(3)^\circ$  in **6** (Table 3, entry 9). The trend is reversed for entry 12 in Table 3. This deviation represents a movement of C(5C) away from precise 2-fold symmetry with C(5B) and is caused by the presence of the bulky Ru(cymene)<sup>2+</sup> substituent on ring A.

In terms of intermolecular distances, interesting short contacts are observed from the sulfur atom of the coordinated ring, S(1A), to the oxygen atoms of one of the  $\text{CF}_3\text{SO}_3^-$  anions, resulting in a pair of triflate anions bridging between two symmetry equivalent host cations, S(1A)–O(1E) 2.922 Å, S(1A)–O(3E) 3.078 Å. This observation is consistent with a high degree of partial positive charge on the coordinated S atom and, hence, strong S–anion electrostatic interactions. In contrast to previous complexes of CTV and calix[4]arene,<sup>12,15,16,26</sup> however, this interaction is of the “end on” type, as opposed to attraction of the anion to all of the atoms of the coordinated ring, presumably as a consequence of the sterically hindered approach to the coordinated carbon atoms.

The crystal structure of the bimetallic complex **9** exhibits an extremely similar conformation to the free ligand **4** without the small deviation noted for **6**, Figure 5 (intercentroid separations; rings A–B 4.81 Å, A–C 4.48 Å, and B–C 4.50 Å; where ring A is defined as containing atoms S(1A)–C(4A), ring B S(1B)–C(4B), and ring C S(1C)–C(4C)). Presumably, the distortions caused by the two metal centers cancel one another out, Table 3. Again, the saddle conformation precludes intracavity anion binding. The presence of a noncrystallographic 2-fold axis passing through S(1C) and C(5B) is consistent with the observation of a singlet signal for the methylene protons of C(5B) in the solution  $^1\text{H}$  NMR spectrum. As with complex **6**, Ir–S distances are consistent with an  $\eta^5$ -coordination of the thiophene rings and a lengthening of two of the S–C bonds in the coordinated rings is observed, S(1B)–C(1B) 1.773(19) Å, S(1A)–C(1A) 1.794(15) Å. Large distortions in the bond angles at the methylene bridges are also evident, with the angle subtended at C(5A) of  $119.6(13)^\circ$  being particularly remarkable.

(21) Atwood, J. L.; Zhang, H. *J. Crystallogr. Spectrosc.* **1990**, *20*, 465–470.

(22) Nishioka, T.; Isobe, K. *Chem. Lett.* **1994**, 1661.

(23) Angelici, R. J. *Acc. Chem. Res.* **1988**, *21*, 387–394.

(24) Fagan, P. J.; Ward, M. D.; Calabrese, J. C. *J. Am. Chem. Soc.* **1989**, *111*, 1698–1719.

(25) Chen, J.; Angelici, R. J. *Organometallics* **1989**, *8*, 2277–2279.

(26) Steed, J. W.; Juneja, R. K.; Atwood, J. L. *Angew. Chem., Int. Ed. Engl.* **1994**, *33*, 2456–2457.

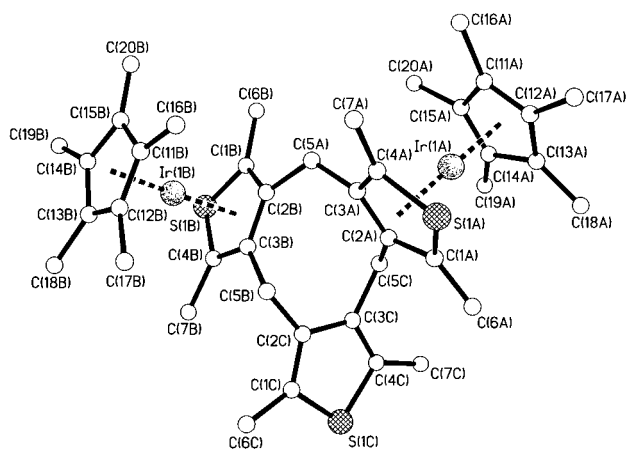
**Table 2. Crystallographic Data for 4, 6, 9, and 11**

	<b>4</b>	<b>6</b>	<b>9</b>	<b>11</b>
empirical formula	C <sub>21</sub> H <sub>24</sub> S <sub>3</sub>	C <sub>33</sub> H <sub>38</sub> F <sub>6</sub> O <sub>6</sub> RuS <sub>5</sub>	C <sub>48</sub> H <sub>61</sub> F <sub>12</sub> Ir <sub>2</sub> NO <sub>13</sub> S <sub>7</sub>	C <sub>70</sub> H <sub>91</sub> B <sub>4</sub> F <sub>16</sub> N <sub>5</sub> Ru <sub>2</sub>
fw	372.58	906.00	1696.80	551.86
temp (K)	293(2)	160(2)	160(2)	173(2)
cryst syst	monoclinic	triclinic	monoclinic	monoclinic
space group	<i>P</i> 2 <sub>1</sub> / <i>c</i>	<i>P</i> $\bar{1}$	<i>C</i> <i>c</i>	<i>P</i> 2 <sub>1</sub> / <i>c</i>
cryst dimens (mm)	0.4 × 0.1 × 0.1	0.5 × 0.3 × 0.1	0.8 × 0.3 × 0.1	0.2 × 0.1 × 0.03
unit cell dimens				
<i>a</i> (Å)	10.2310(5)	10.1661(12)	20.6686(16)	16.0574(8)
<i>b</i> (Å)	5.2960(2)	13.6994(17)	17.4490(13)	11.6582(6)
<i>c</i> (Å)	34.4670(14)	14.3077(17)	17.0768(13)	19.7603(5)
$\alpha$ (deg)	90	71.267(3)	90	90
$\beta$ (deg)	94.182(1)	86.181(3)	106.158(2)	102.577(1)
$\gamma$ (deg)	90	88.430(3)	90	90
<i>V</i> (Å <sup>3</sup> )	1862.57(14)	1882.8(4)	5915.4(8)	3610.4(3)
<i>Z</i>	4	2	4	2
<i>D<sub>c</sub></i> (g cm <sup>-3</sup> )	1.329	1.598	1.905	1.428
$\mu$ (mm <sup>-1</sup> )	0.398	0.766	4.840	0.504
max, min transmission	n/a	0.875, 0.608	0.379, 0.241	0.985, 0.906
<i>F</i> (000)	792	924	3336	1596
$\theta$ range (deg)	4.03–25.00	1.51–28.35	1.55–25.00	3.62–25.00
no. of reflns coll'd	25 828	14 630	15 221	31 329
no. of indep reflns	3224	8279	7144	6004
<i>R</i> (int)	0.0530	0.0190	0.0398	0.0790
data/params	3224/218	8279/470	7144/801	6004/446
goodness-of-fit on <i>F</i> <sup>2</sup>	1.026	1.056	1.049	1.070
<i>R</i> indices, <i>F</i> <sup>2</sup> > 2 $\sigma$ ( <i>F</i> <sup>2</sup> )	<i>R</i> 1 = 0.0454	<i>R</i> 1 = 0.0311	<i>R</i> 1 = 0.0479	0.0484
<i>R</i> indices (all data, <i>F</i> <sup>2</sup> )	w <i>R</i> 2 = 0.1240	w <i>R</i> 2 = 0.0757	w <i>R</i> 2 = 0.1290	0.1319
largest diff peak/hole (e Å <sup>-3</sup> )	0.233/–0.242	0.756/–0.648	2.860/–2.524 (close to Ir)	0.706/–0.691

**Table 3. Torsion Angles (deg) about the Methylene Bridges for 4, 6, and 9<sup>a</sup>**

entry	torsion angle (4 and 6)	<b>4</b>	<b>6</b>	torsion angle (9)	<b>9</b>
1	C(2A)–C(3A)–C(5A)–C(2B)	110.5(2)	103.4(2)	C(3A)–C(2A)–C(5C)–C(3C)	106.5(16)
2	C(4A)–C(3A)–C(5A)–C(2B)	–67.1(3)	–75.3(3)	C(1A)–C(2A)–C(5C)–C(3C)	–72.9(16)
3	C(3A)–C(5A)–C(2B)–C(1B)	125.3(2)	121.7(2)	C(2A)–C(5C)–C(3C)–C(4C)	125.5(16)
4	C(3A)–C(5A)–C(2B)–C(3B)	–52.9(3)	–58.0(3)	C(2A)–C(5C)–C(3C)–C(2C)	–48.9(17)
5	C(2B)–C(3B)–C(5B)–C(2C)	–62.3(3)	–49.5(3)	C(3C)–C(2C)–C(5B)–C(3B)	–56.1(17)
6	C(4B)–C(3B)–C(5B)–C(2C)	116.8(2)	125.7(2)	C(1C)–C(2C)–C(5B)–C(3B)	122.5(16)
7	C(3B)–C(5B)–C(2C)–C(1C)	–78.3(3)	–64.7(3)	C(2C)–C(5B)–C(3B)–C(4B)	–66.3(18)
8	C(3B)–C(5B)–C(2C)–C(3C)	103.0(2)	110.6(2)	C(2C)–C(5B)–C(3B)–C(2B)	107.6(15)
9	C(2C)–C(3C)–C(5C)–C(2A)	–10.5(4)	–59.2(3)	C(3B)–C(2B)–C(5A)–C(3A)	–9(4)
10	C(4C)–C(3C)–C(5C)–C(2A)	170.0(2)	124.4(2)	C(1B)–C(2B)–C(5A)–C(3A)	160.4(18)
11	C(1A)–C(2A)–C(5C)–C(3C)	127.3(3)	167.9(2)	C(2B)–C(5A)–C(3A)–C(4A)	133.1(19)
12	C(3A)–C(2A)–C(5C)–C(3C)	–57.0(3)	–8.9(4)	C(2B)–C(5A)–C(3A)–C(2A)	–56(3)

<sup>a</sup> The numbering scheme adopted for **9** is consistent that adopted for **2**<sup>15</sup> in that rings A and B are the metal-bearing ones. This results in ring C laying on the pseudo-2-fold axis, as opposed to ring B in **4** and **6**.

**Figure 5.** X-ray crystal structure of the bimetallic cation in **9** showing the saddle conformation for the ligand **4**.

While the pronounced saddle conformation does not result in a molecular cavity, a region of void space between the two C<sub>5</sub>Me<sub>5</sub> rings is occupied by a disordered molecule of dmf. As in the case of **6**, the triflate anions in **9** make short contacts to the coordinated sulfur atoms S(1A)–O(3G) and –O(3D) 3.068 and 3.448 Å, respec-

tively; S(1B)–O(3D), –O(1E), and –O(3G) 3.036, 3.264, and 3.348 Å, resulting in O(3D) and O(3G) forming bridges between S(1A) and S(1B). A search out to 3.6 Å revealed no short contacts to S(1C), consistent with the fact that this atom is not metalated.

**Solution Studies.** The absence of a bowl-shaped molecular cavity in hosts of type **6**, **7**, and **9** suggests that it may be worthwhile to compare their anion-binding ability with CTV-based species such as **2**. Accordingly, <sup>1</sup>H NMR titration studies were carried out on the bimetallic host complexes **2** and **9** in a variety of solvents.

In water, problems were encountered with hydrolysis and precipitation of both hosts, precluding calculation of accurate binding constants. However, for **2**, addition of NaBr resulted in significant changes in the chemical shift of many of the signals in the <sup>1</sup>H NMR spectrum. In particular, the low-field resonance assigned to the protons of the coordinated aromatic rings of the CTV shifted from  $\delta$  7.69 to 7.91 ppm upon addition of 10 equiv of anion. Little further change was observed up to a 100:1 Br<sup>–</sup>:host mole ratio. Addition of up to 10 equiv of NaBr to an aqueous solution of **9** resulted in

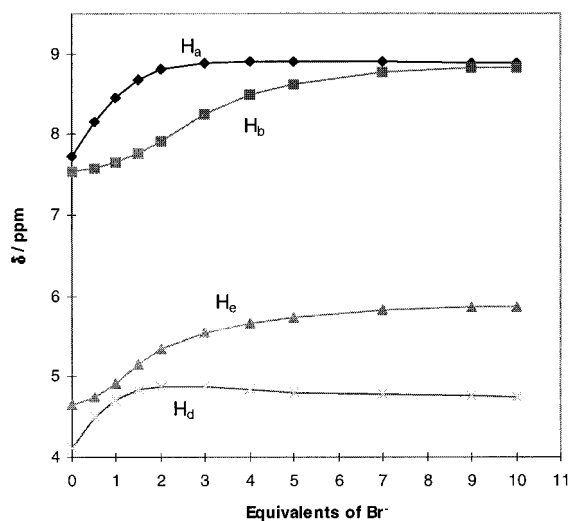
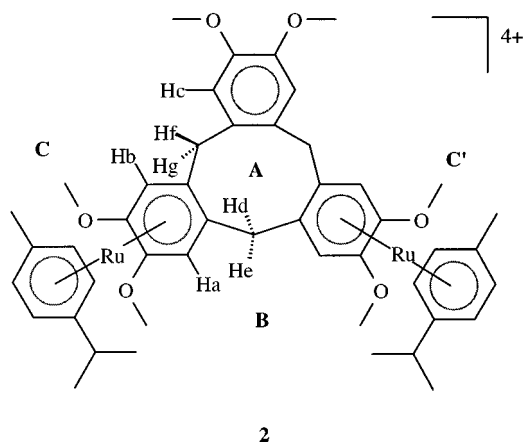


**Figure 6.** Variation of the chemical shift of the protons of **2** on addition of  $\text{Br}^-$  in nitromethane solution.

virtually no change. Further studies were prevented by precipitation of the complex. The possibility that the observed shifts arise as a consequence of the changing ionic strength of the solution were ruled out by an analogous experiment with  $\text{NaCF}_3\text{SO}_3$ , which did not result in any changes to the spectrum.

In a less polar solvent,  $\text{NO}_2\text{Me}-d_3$ , large changes in the resonances assigned to the protons of the coordinated CTV rings of host **2** were observed in  $\text{NO}_2\text{Me}-d_3$  solution upon addition of  $[\text{NBu}_4]\text{X}$  ( $\text{X} = \text{Cl}^-$ ,  $\text{Br}^-$ ,  $\text{I}^-$ ,  $\text{H}_2\text{PO}_4^-$ ). The resulting titration curves for various CTV protons with  $\text{X} = \text{Br}^-$  are shown in Figure 6. In all cases, two types of behavior were observed within the same set of spectra, depending on the proximity of the proton monitored to the various binding sites. In the first case, the rapid 1.2 ppm change in the chemical shift of  $\text{H}_a$  is virtually complete after addition of 2 equiv of  $\text{Br}^-$ , suggesting the initial formation of a 2:1 complex, probably involving anion binding at sites **A** and **B** (Figure 6) which are situated between the pair of metal centers. The slower change in the chemical shift of  $\text{H}_b$  suggests a secondary type of complex formation of a lower binding constant involving sites **C** and **C'**. The two kinds of behavior exemplified by  $\text{H}_a$  and  $\text{H}_b$  are also seen in the signals for the rest of the CTV protons with those in close proximity to sites **A** and **B** exhibiting a similar behavior to  $\text{H}_a$  (e.g.  $\text{H}_d$ ) and those nearer to sites of type **C** resembling the behavior of  $\text{H}_b$  (e.g.  $\text{H}_e$ ). Very

**Table 4.**  $^1\text{H}$  NMR Titration Data for the Interaction of **2** with Anions

anion	$\Delta\delta$ (ppm) (after 10 equiv of anion)	$K_1$ ( $\text{M}^{-1}$ )
$\text{Cl}^-$	1.40	$1.25(7) \times 10^3$
$\text{Br}^-$	1.21	$1.07(3) \times 10^3$
$\text{I}^-$	0.89	$0.85(5) \times 10^3$

similar behavior was observed for both  $\text{Cl}^-$  and  $\text{I}^-$ , with the maximum chemical shift change being observed for  $\text{Cl}^-$  and the minimum for  $\text{I}^-$ , suggesting a selectivity sequence of  $\text{Cl}^- > \text{Br}^- > \text{I}^-$ . Binding constants for the complexation of the first anion (intracavity binding) were obtained from the data for  $\text{H}_a$  using the program EQNMR,<sup>27</sup> Table 4. The preference for  $\text{Cl}^-$  over the larger halides may be readily rationalized on the basis of electrostatic arguments, with the smaller  $\text{Cl}^-$  anion presumably nestling deeply between the two ruthenium centers. As a control, an analogous titration was carried out with  $[\text{NBu}_4][\text{CF}_3\text{SO}_3]$ , which resulted in no changes whatsoever to the spectrum. The preference exhibited for sites **A** and **B** over **C** is consistent with the fact that site **C** is adjacent to only one metal center. This result is consistent with those obtained for the calix[4]arene host  $[\{\text{Ru}(\eta^6\text{-}p\text{-cymene})\}_4(\eta^6:\eta^6:\eta^6:\eta^6\text{-calix[4]arene-2H})]^{6+}$  (**10**) in which the  $K_1$  values (in water) were generally found to be at least an order of magnitude larger than  $K_2$  as a consequence of the fact that the intracavity binding site is adjacent to all four metal centers.<sup>12</sup> In general, the magnitudes of  $K_1$  for all of the halides in the case of **2** are much larger than those observed for **10** in aqueous solution (551, 133 and  $51 \text{ M}^{-1}$  for binding of  $\text{Cl}^-$ ,  $\text{Br}^-$ , and  $\text{I}^-$ , respectively) and highlights the effect of the less competitive solvent.

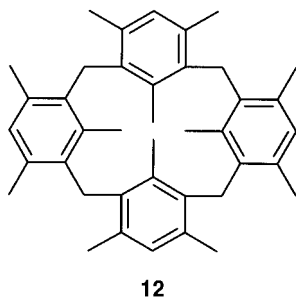
The analogous NMR titration with  $\text{H}_2\text{PO}_4^-$  was frustrated by the resulting complex's extreme insolubility, with complete precipitation observed even in the presence of only 2 equiv of  $\text{H}_2\text{PO}_4^-$ . However, the downfield chemical shift change at lower concentrations of the resonance assigned to  $\text{H}_a$  is again consistent with strong interaction with the anion, as expected given the preference of host **2** for other tetrahedral oxyanions such as  $^{99}\text{TcO}_4^-$ .<sup>15,16</sup>

In contrast, addition of 1–1000 equiv of  $[\text{NBu}_4]\text{Br}$  to host **9** in  $\text{NO}_2\text{Me}-d_3$  resulted in very few changes to the spectrum. The doublet resonance  $\text{H}_a$  (analogous to  $\text{H}_f$  in complex **2**) at  $\delta$  3.93 ppm was observed to shift to 3.84 ppm in the presence of 10 equiv of anion but changed little thereafter. No change whatsoever was observed in the chemical shift of singlet  $\text{H}_b$  (analogous to  $\text{H}_d$  and  $\text{H}_e$  in **2**). This is surprising since even in the absence of a molecular cavity, anion binding external to the cavity between the two metal centers might be expected by analogy with **2**. It can be seen in the X-ray crystal structure of **9** (Figure 5), however, that this site is extremely sterically hindered and is occupied by a dmf solvent molecule in the solid state.

Finally, the ability of host **9** to bind  $\text{Br}^-$  was also examined in an even less polar solvent acetone. In this case, a significant response was obtained on addition of  $[\text{NBu}_4]\text{Br}$ , with the signal assigned to  $\text{H}_b$  shifting from 4.50 ppm in the absence of  $\text{Br}^-$  to 5.13 ppm after addition of 10 equiv of anion. Similarly, a shift of 0.34

ppm was noted for the protons H<sub>a</sub>. Solubility constraints did not allow sufficient data to be collected to calculate reliable binding constants.

**Calixarene Conformations.** In our previous work with calix[4]arene derivatives,<sup>12</sup> we focused almost exclusively on the bowl conformation. In view of the results obtained above for hosts **2** and **9**, we decided to investigate the possibility of anion binding using calixarene-based organometallic hosts in other conformations. To this end, [ $\{\text{Ru}(\eta^6\text{-}p\text{-cymene})\}_2(\eta^6\text{:}\eta^6\text{-C}_{46}\text{H}_{48})\text{]BF}_4$ ] (11), based on the mesityl calix[4]arene **12**, was



prepared in 79% yield using a procedure analogous to that for **6**. Calixarene **12** has been studied little but is thought to exist exclusively in the 1,3-alternate form as a consequence of an unfavorable steric interaction between the upper-rim methyl substituents and the lack of hydroxyl functionalities to stabilize the cone conformation.<sup>28</sup>

<sup>1</sup>H NMR titration experiments with [NBu<sub>4</sub>]Br, in an analogous manner to **2**, resulted in the striking observation that the calixarene proton H<sub>a</sub> shifted markedly downfield ( $\Delta\delta = 0.47$  ppm after addition of 10 equiv of Br<sup>-</sup>, rising to 0.74 ppm after 100 equiv) while the chemical shift of the protons attached to the uncoordinated decks remained virtually unchanged, suggesting binding at or near the molecular cleft running between the two coordinated aromatic rings of the calixarene. The relatively small binding constant of 76(12) M<sup>-1</sup>, however, indicates that there is little or no cooperativity between the two metal centers in the complex. Analogous experiments with Cl<sup>-</sup> and I<sup>-</sup> gave  $\Delta\delta$  values of 0.60 and 0.15 ppm, respectively, after addition of 10 equiv of anion, suggesting the selectivity sequence Cl<sup>-</sup> > Br<sup>-</sup> > I<sup>-</sup>, again consistent with electrostatic control of the binding.

X-ray crystallographic analysis of host **11** proved difficult as a consequence of the complex's strong tendency to co-crystallize with large numbers of solvent molecules, with consequent crystal instability toward desolvation. Eventually, a structure of the acetonitrile solvate [ $\{\text{Ru}(\eta^6\text{-}p\text{-cymene})\}_2(\eta^6\text{:}\eta^6\text{-C}_{40}\text{H}_{48})\text{]BF}_4\cdot\text{MeCN}$ ] was obtained at -100 °C, Figure 8. Even at this low temperature the acetonitrile proved to be highly disordered, occupying extensive channels running between the clefts caused by the nearly parallel faces of the calixarene aromatic rings. One-half of the metal complex is found in the asymmetric unit. Both unique tetrafluoroborate anions are situated externally to the molecular cleft between the two metal centers, with one face onto the *p*-cymene ligand while the other, interest-

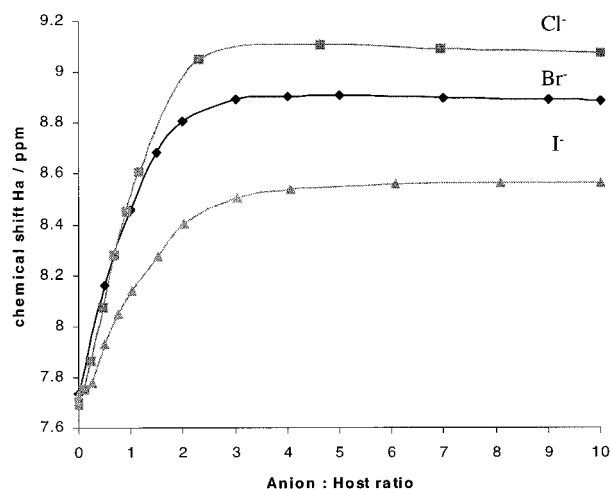


**Figure 7.** Variation in the chemical shift of H<sub>a</sub> on addition of various anions.

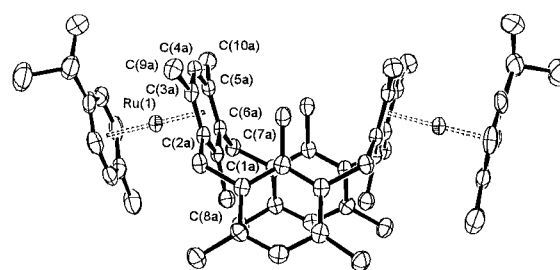


**Figure 8.** X-ray crystal structure of the 1,3-alternate calixarene complex [ $\{\text{Ru}(\eta^6\text{-}p\text{-cymene})\}_2(\eta^6\text{:}\eta^6\text{-C}_{40}\text{H}_{48})\text{]BF}_4\cdot 5\text{MeCN}$  (**11**).

ingly, is directly above the coordinated calixarene ring; C(4A)⋯F(3B) 3.28(2) Å. The close contact between this calixarene C–H unit and the anion, thus, accounts for the observed solution data, with binding occurring *above* the calixarene cavity involving a relatively strong C–H⋯anion hydrogen-bonding interaction as a consequence of the increased acidity of the CH proton upon coordination to the metal center. This results in significant chemical shift changes only to the proton attached to C(4A) and those of the nearby *p*-cymene ring and not the nonmetalated ring C(4B). Clearly, however, in contrast to **2** and **10**, no cooperative effects exist between the two metal centers to enhance binding.

## Conclusions

It has been demonstrated that the widely disparate anion-binding selectivities of complexes **2** and **9** may be a consequence of the very different conformations of the macrocyclic core which, in the case of **2**, provides convenient, readily accessible binding sites for anions such as Br<sup>-</sup>. For **9**, there is no readily accessible cavity or cleft as a consequence of the bulky C<sub>5</sub>Me<sub>5</sub><sup>-</sup> ligands and the highly twisted conformation of the macrocyclic ligand, resulting in very limited anion affinity. This result highlights the influence of molecular shape on host–guest properties and suggests the possibility of designed anion selectivity by careful control of host size and shape. As noted in previous work,<sup>15</sup> significant influence is also exerted by the solvent on anion-binding properties. In the case of **11**, steric factors result in an unusual anion-binding mode and the observation of a

(28) Bottino, F.; Montaudo, G.; Maravigna, P. *Ann. Chim. (Rome)* **1967**, *57*, 972.

relatively strong C—H···anion hydrogen-bonding interaction.

## Experimental Section

**Instrumentation.** Mass spectra were run at King's College London in FAB mode in a thioglycerol matrix. NMR spectra were recorded on Bruker ARX-360 and AMX-400 spectrometers at King's College, and we thank the ULIRS NMR service for running these spectra. Microanalyses were performed at University College London. All manipulations except for the synthesis of the starting materials and where indicated were carried out in air, and the products showed no oxygen sensitivity or chemical instability toward moisture, although bimetallic complexes lost enclathrated solvent molecules when exposed to the atmosphere.

**Materials.** The chloro complexes  $[\{\text{Ru}(\eta^6\text{-}p\text{-cymene})\text{Cl}(\mu\text{-Cl})\}_2]$  (**5**)<sup>29</sup> and  $[\{\text{Ir}(\text{Cp}^*)\text{Cl}(\mu\text{-Cl})\}_2]$  (**8**)<sup>20</sup> and ligand **4**<sup>18</sup> were prepared according to published literature procedures. Ruthenium and iridium trichloride hydrates were obtained from Johnson Matthey plc, and  $\text{RuCl}_3 \cdot x\text{H}_2\text{O}$  ( $x = \text{ca. } 2$ ) was purified before use by repeated dissolution in water and boiling to dryness. All other reagents and materials were obtained from the usual commercial sources.

**Preparations.**  $[\{\text{Ru}(\eta^6\text{-}p\text{-MeC}_6\text{H}_4\text{CHMe}_2)(\eta^5\text{-C}_{21}\text{H}_{24}\text{S}_3)\}][\text{CF}_3\text{SO}_3]_2$  (**6**). Complex **5** (0.15 g, 0.24 mmol) was treated with  $\text{Ag}[\text{CF}_3\text{SO}_3]$  (0.25 g, 0.98 mmol) in acetone (30 cm<sup>3</sup>) for 15 min. The mixture was filtered through Celite, and the solvent was evaporated in vacuo. The resulting orange oil was dissolved in  $\text{CF}_3\text{CO}_2\text{H}$  (40 cm<sup>3</sup>) and refluxed under nitrogen with ligand **4** (0.18 g, 0.49 mmol) for 25 h. The resulting blue-green solution was diluted with diethyl ether until incipient precipitation, and the mixture was allowed to stand at  $-4^\circ\text{C}$  for 24 h, resulting in the formation of the product as large brown needles. Yield: 0.36 g, 0.40 mmol, 82%. Anal. Calcd for  $\text{C}_{33}\text{H}_{38}\text{F}_6\text{O}_6\text{RuS}_5$ : C, 43.75; H, 4.23; S, 17.69. Found: C, 43.10; H, 4.05; S, 17.15.

$[\{\text{Ru}(\eta^6\text{-}p\text{-MeC}_6\text{H}_4\text{CHMe}_2)\}_2(\eta^5\text{-}\eta^5\text{-C}_{21}\text{H}_{24}\text{S}_3)] [\text{CF}_3\text{SO}_3]_4$  (**7**). Complex **5** (0.21 g, 0.34 mmol) was treated with  $\text{Ag}[\text{CF}_3\text{SO}_3]$  (0.35 g, 1.36 mmol) in acetone followed by refluxing with ligand **4** (0.08 g, 0.22 mmol) for 12 h in  $\text{CF}_3\text{CO}_2\text{H}$  as for **6**. The resulting brown solution was diluted with diethyl ether to give the product as a brown precipitate, which was shown to contain a significant quantity of  $\text{CF}_3\text{CO}_2\text{H}$  by <sup>1</sup>H NMR spectroscopy. Attempts to dry the compound resulted in partial decomposition to **6**. Yield: 0.34 g, 0.19 mmol, 86%. Anal. Calcd for  $\text{C}_{33}\text{H}_{38}\text{F}_6\text{O}_6\text{RuS}_5 \cdot 2\text{CF}_3\text{CO}_2\text{H} \cdot 5\text{H}_2\text{O}$ : C, 33.50; H, 3.65; S, 12.75. Found: C, 32.85; H, 3.50; S, 13.35.

$[\{\text{Ir}(\eta^5\text{-C}_5\text{Me}_5)\}_2(\eta^5\text{-}\eta^5\text{-C}_{21}\text{H}_{24}\text{S}_3)] [\text{CF}_3\text{SO}_3]_4$  (**9**).  $[\{\text{Ir}(\eta^5\text{-C}_5\text{Me}_5)\text{Cl}(\mu\text{-Cl})\}_2]$  (**8**; 0.43 g, 0.54 mmol) was treated with  $\text{Ag}[\text{CF}_3\text{SO}_3]$  (0.55 g, 2.13 mmol) in acetone followed by refluxing with ligand **4** (0.10 g, 0.27 mmol) for 19 h in  $\text{CF}_3\text{CO}_2\text{H}$  as for **6**. The resulting brown solution was diluted with diethyl ether to give the product. Yield: 0.39 g, 0.20 mmol, 72%. Anal. Calcd for  $\text{C}_{45}\text{H}_{54}\text{F}_{12}\text{O}_{12}\text{Ir}_2\text{S}_7 \cdot 5\text{Et}_2\text{O}$ : C, 39.15; H, 5.25; S, 11.25. Found: C, 39.60; H, 4.10; S, 11.25. Crystals suitable for X-ray crystal structure determination were prepared by slow diffusion of diethyl ether into a dmf solution to give colorless crystals of the product as the dmf solvate.

$[\{\text{Ru}(\eta^6\text{-}p\text{-MeC}_6\text{H}_4\text{CHMe}_2)\}_2(\eta^6\text{-}\eta^6\text{-C}_{40}\text{H}_{48})] [\text{BF}_4]_4$  (**11**). Complex **5** (0.15 g, 0.24 mmol) was treated with  $\text{Ag}[\text{BF}_4]$  (0.21 g, 1.08 mmol) in acetone followed by refluxing with ligand **12** (0.23 g, 0.43 mmol) for 12 h in  $\text{CF}_3\text{CO}_2\text{H}$  as for **6**. The resulting brown-orange solution was filtered to remove unreacted calixarene and then diluted with diethyl ether to give the product as a white precipitate, which was shown to contain a significant quantity of  $\text{CF}_3\text{CO}_2\text{H}$  by <sup>1</sup>H NMR spectroscopy. Yield: 0.30 g, 0.19 mmol, 79%. Anal. Calcd for  $\text{C}_{60}\text{H}_{76}\text{B}_4\text{F}_{16}\text{Ru}_2 \cdot 2\text{CF}_3\text{CO}_2\text{H}$ : C, 48.85; H, 4.50. Found: C, 49.55; H, 5.15.

**4,6,10,12,16,18,22,24,25,26,27,28-Dodecamethylpentacyclo[19.3.1.1.3.71.9.13.15.19]octacosane-1(25),3,5,7(28),9,11,13-(27),15,17,19(26),21,23-dodecaene (12).** The compound was prepared by a modification of the literature procedure.<sup>28</sup> To a solution of  $\alpha^2$ -chloroisodurene (5.00 g, 29.7 mmol) in dry  $\text{CH}_2\text{-Cl}_2$  (50 cm<sup>3</sup>) was added  $\text{SnCl}_4$  (0.7 cm<sup>3</sup>) under a constant stream of  $\text{N}_2$ . The mixture was refluxed for 2 h, resulting in a color change to red and subsequent formation of a white precipitate. The mixture was carefully hydrolyzed with water (50 cm<sup>3</sup>) and then extracted with two further portions of  $\text{CH}_2\text{Cl}_2$  (25 cm<sup>3</sup> each). The extract was dried with anhydrous  $\text{MgSO}_4$ , and the volume was reduced in vacuo, resulting in the deposition of the product as a white solid. Yield: 3.88 g, 7.34 mmol, 98%.

**Solution Studies.** Stock solutions (generally  $2.5 \times 10^{-3}$  M) of host complex were prepared in  $\text{D}_2\text{O}$ ,  $\text{NO}_2\text{Me-}d_3$ , or acetone-*d*<sub>3</sub>. To 0.3 cm<sup>3</sup> of this host solution was added increasing amounts of 0.25 M solutions of the anion as the tetrabutylammonium salt (organic solvents) or the sodium salt (water) in the same solvent in a 5 mm NMR tube, and the volume was topped off to a total of 0.6 cm<sup>3</sup> with fresh solvent. For very high anion:host ratios, 2.5 M anion solutions were used in the same way. <sup>1</sup>H NMR spectra were recorded in the usual way for ca. 10–15 samples, and the resulting titration curve was analyzed by the EQNMR software.<sup>27</sup>

**Crystallography.** Crystal data and data collection parameters are summarized in Table 2. In the case of compounds **6** and **9**, crystals were mounted using a viscous polyfluorinated hydrocarbon oil on the end of a glass fiber and cooled on the diffractometer. Crystallographic measurements were carried out with a Siemens SMART diffractometer equipped with graphite-monochromated Mo K $\alpha$  radiation ( $\lambda = 0.71073 \text{ \AA}$ ) using  $\omega$  rotations with narrow frames ( $0.3^\circ$ ). Data sets were corrected for Lorentz and polarization effects and for the effects of absorption using a pseudo- $\psi$ -scans method based on comparison of equivalent and repeated data. For compounds **4** and **11**, the crystal was mounted on a glass fiber using a fast setting epoxy resin. A total of 90 oscillation frames of 30 s exposure time (45 s for **11**) with  $2^\circ$  rotation in  $\phi$  were recorded using a Nonius KappaCCD diffractometer, with a detector to crystal distance of 25 mm. The crystal was indexed from the first 10 frames using the DENZO-SMN package,<sup>34</sup> and positional data were refined along with diffractometer constants to give the final unit cell parameters. The data were integrated, scaled, and corrected for Lorentz and polarization effects and for the effects of absorption using the program Scalepack.<sup>34</sup> The structures were solved using the direct methods option of SHELXS-97<sup>30</sup> and developed via alternating least-squares cycles and difference Fourier synthesis (SHELXL-97<sup>30</sup>) with the aid of the program RES2INS.<sup>31</sup> For compounds **6** and **9**, structures were solved by direct (**9**) or Patterson (**6**) methods (SHELXTL<sup>32</sup>) and developed using conventional alternating cycles of least-squares refinement and difference Fourier synthesis (SHELXL-96<sup>33</sup>) on  $F^2$  values. In all cases, all non-hydrogen atoms were refined anisotropically while hydrogen atoms were fixed in idealized positions and allowed to ride on the atom to which they were attached. Hydrogen-atom isotropic displacement parameters were tied to those of the atom to which they were attached (1.2 times that of the carrier atom or 1.5 times for methyl groups). All calculations were carried out on an IBM-PC compatible

(29) Bennett, M. A.; Smith, A. K. *J. Chem. Soc., Dalton Trans.* **1974**, 233–241.

(30) Sheldrick, G. M. *SHELX-97*; University of Göttingen: Göttingen, Germany, 1997.

(31) Barbour, L. J. *RES2INS*; University of Missouri: Columbia, MO, 1995.

(32) Sheldrick, G. M. *Acta Crystallogr., Sect. A* **1990**, *46*, 467.

(33) Sheldrick, G. M. *SHELXL-96*; University of Göttingen: Göttingen, Germany, 1996.

(34) Otwinowski, Z.; Minor, W. In *Methods in Enzymology*; Sweet, R. M., Carter, C. W., Eds.; Academic Press: New York, 1996; Vol. 276, pp 307–326.

personal computer or Silicon Graphics Indy workstation. In the case of compound **9**, disorder was noted in the case of the enclathrated molecule of dmf and was modeled successfully in terms of two positions, each of 50% occupancy, for all of the dmf carbon atoms. The space group  $C2/c$  was considered, but the structure refined considerably less well. The absolute structure parameter was refined to 0.416(13), which additionally suggests the space group  $Cc$  with partial racemic twinning. Restraints were applied to the geometry, the anisotropic displacement parameters for the dmf molecule and to the anisotropic displacement parameters of atoms C13A, O1S, C2A, C20B, C12B, and C15B. For compound **11**, severe disorder of the enclathrated acetonitrile molecules was encountered. After considerable effort a model involving 5 N atom positions and 15 C atom positions (all isotropic) was adopted with occupancies ranging from 0.25 to 1.0.

**Acknowledgment.** We thank Johnson Matthey plc for generous loans of ruthenium trichloride, the Nuffield

Foundation for the provision of computing equipment, and NATO for the award of a Collaborative Research Grant (ref. CRG 960320). We are also grateful to Prof. O. Meth-Cohn for helpful advice on the synthesis of compound **4**. We thank King's College London and the EPSRC for provision of the KappaCCD at King's College London and the EPSRC for provision of the diffractometer in Newcastle (grant awarded to Prof. W. Clegg whom we thank for use of this and associated crystallographic facilities).

**Supporting Information Available:** Tables of crystal data, atomic coordinates, bond lengths and angles, anisotropic displacement parameters, hydrogen atoms, and interbond torsion angles (38 pages). Ordering information is given on any current masthead page.

OM970739Q